GROWTH OF SHORT FATIGUE CRACKS FROM STRESS CONCENTRATIONS IN N18 SUPERALLOY

F. SANSOZ [1,2], B. BRETHES [3] and A. PINEAU [1]

(1) Centre des Matériaux, UMR 7633 CNRS, Ecole des Mines de Paris, B.P. 87, 91003 Evry cedex, France
(2) Currently at: Mechanics of Materials Laboratory, Department of Mechanical Engineering, University of Rhode Island, Kingston, RI 02881, USA
(3) SNECMA, Etablissement de Villaroche, 77550 Moissy Cramayel, France

ABSTRACT

DEN notched specimens containing a small semi-circular slot (0.1 mm) were made of a powder-metallurgy Ni base superalloy, alloy N18, in order to study the growth of short fatigue cracks from a stress concentration. Fatigue crack growth tests were conducted at 650°C with trapezoidal cycles 10s-300s-10s. Typical downtrends of crack growth rates were observed in these specimens during the crack propagation. Non-uniform stress and strain gradients at the notch root were calculated by FEM modelling using viscoplastic constitutive equations. The stress intensity factor was determined using these profiles and a weight-function method. To account for crack closure effects, a methodology was developed to calculate the effective stress intensity factor in the crack depth and at the free surface of notched specimens. It is shown that, for small crack lengths, in-depth opening ratios are significantly less pronounced in notched specimens than in unnotched specimens. Moreover, the crack closure effect determined at the free surface is higher than that calculated in-depth. The effect of a notch on this difference is addressed. Using these calculations, it is shown that the differences in crack growth rates observed between short and long cracks are no longer existent when crack closure effects are properly considered.

KEYWORDS

Short fatigue cracks, notch plasticity effects, crack closure, Finite Element calculations, 3D analytical predictions, powder metallurgy superalloy.

INTRODUCTION

Since powder metallurgy superalloys are used in the manufacturing of turbine disks for aeroengines, a clear understanding of the notch effects is required for a good assessment of defect tolerance at elevated temperature. One of these superalloys, N18 alloy, exhibits an excellent mechanical strength and good fatigue and creep resistances up to 650°C. However, during the processing route, a very small amount of inclusions are carried in the material. The size of the biggest inclusions is no more than 100 μm, but a small semi-elliptical crack could eventually be initiated under stress concentrations such as blade fixtures. Furthermore, due to high service temperatures, strongly non-uniform viscoplastic stress and strain fields are

developed in the vicinity of these notches. The objective is, therefore, to take into account the notch plasticity effects in the growth behaviour of these semi-elliptical fatigue cracks.

In unnotched specimens, Pearson [1] showed differences in growth between physically small cracks (< 0.5 mm) and long cracks (> 0.5 mm). In order to correlate these differences, a number of authors developed the concept of intrinsic threshold [2]. In this approach, it is considered that the range of applied load is smaller than the stress intensity range, $\Delta K = K_{max} - K_{min}$, and is equal to $\Delta K_{eff} = K_{max} - K_{op}$, where K_{op} is the opening stress intensity factor calculated when the crack is fully opened [3]. Furthermore, in the case of short cracks, the determination of the effective stress intensity range ΔK_{eff} is strongly dependent of the crack length. On the other hand, Smith and Miller [4] investigated the behaviour of physically small cracks emanating from notches. Due to the notch plasticity effects, the load applied far from the notch can not be directly used and a local approach must be considered to determine the stresses within the notch. This approach was used successfully in several studies [5,6] in which crack closure effects were shown to significantly reduce the crack growth rates differences observed between short and long cracks. More recently Pommier et al. [7,8] have tested N18 alloy at 650°C. These authors showed that stress relaxation effects occurring at notch root can largely modify the effective stress intensity factor ΔK_{eff} when the crack is small in length (< 0.5 mm). Besides, on René 95 alloy, a methodology [9] was suggested to combine both the notch plasticity effects and the in-depth and the surface growth of penny-shaped cracks. However, the determination of the crack closure effect along the front of semi-elliptical cracks has not been fully investigated, in particular when creep-fatigue loading and notch plasticity effects are both considered. These objectives are partly achieved in this study by proposing a methodology to calculate the effective stress intensity range, ΔK_{eff}, in-depth and at the free surface of semi-elliptical cracks. The role of notch plasticity under creep-fatigue loading is addressed. This methodology is then applied to correlate the crack growth rates of short fatigue cracks measured on N18 alloy with Double-Edge-Notched specimens, specifically designed to study the effect of a stress gradient on the behaviour of small cracks.

MATERIAL AND EXPERIMENTS

Material and experimental procedure

N18 alloy is a Ni based superalloy. Its chemical composition is: Ni - 11.5% Cr - 15.7% Co - 6.5% Mo - 4.35% Al - 4.35% Ti - 0.5% Hf (weight %). All tests were performed on a “bulk” microstructure, which is obtained through a specific heat treatment procedure given elsewhere [10,11]. The monotonic and cyclic yield stresses at 650°C are 1050 MPa and 1150 MPa respectively. For a more comprehensive overview on this alloy, see reference [10].

Fatigue tests were carried out on Double-Edge-Notched (DEN) geometry containing two symmetrical U-shaped notches. The notch root radius is 2 mm and the reduced cross-section is 5 x 10 mm^2. A microstructural defect is simulated by a small semicircular EDM slot of 0.1 mm in depth located at the centre of the notch root on one side of the specimen. This machined defect is shown in Fig. 1.a. No precracking is made on the DEN specimens and the crack length on the free surface of the specimen is measured up to 1 mm from the initial semi-circular defect (0.1 mm). Tests were performed at 650°C with trapezoidal cycles 10s-300s-10s, maintaining a hold time of 5 min at maximum applied load. These specimens were tested with a constant nominal stress S_{max} varying from 600 MPa to 900 MPa, which represent respectively 0.5 and 0.8 times the monotonic yield strength (σ_0), and load ratios equal to 0, -0.5 or -1. A

high-resolution optical system (Questar) was used to measure crack lengths at the free surface of specimen in the notch bottom. This technique has proved to be efficient to detect *in-situ* half-surface crack increments as small as 10 μm, while a conventional Potential Drop method is not enough sensitive to measure the length of very small cracks [11,12].

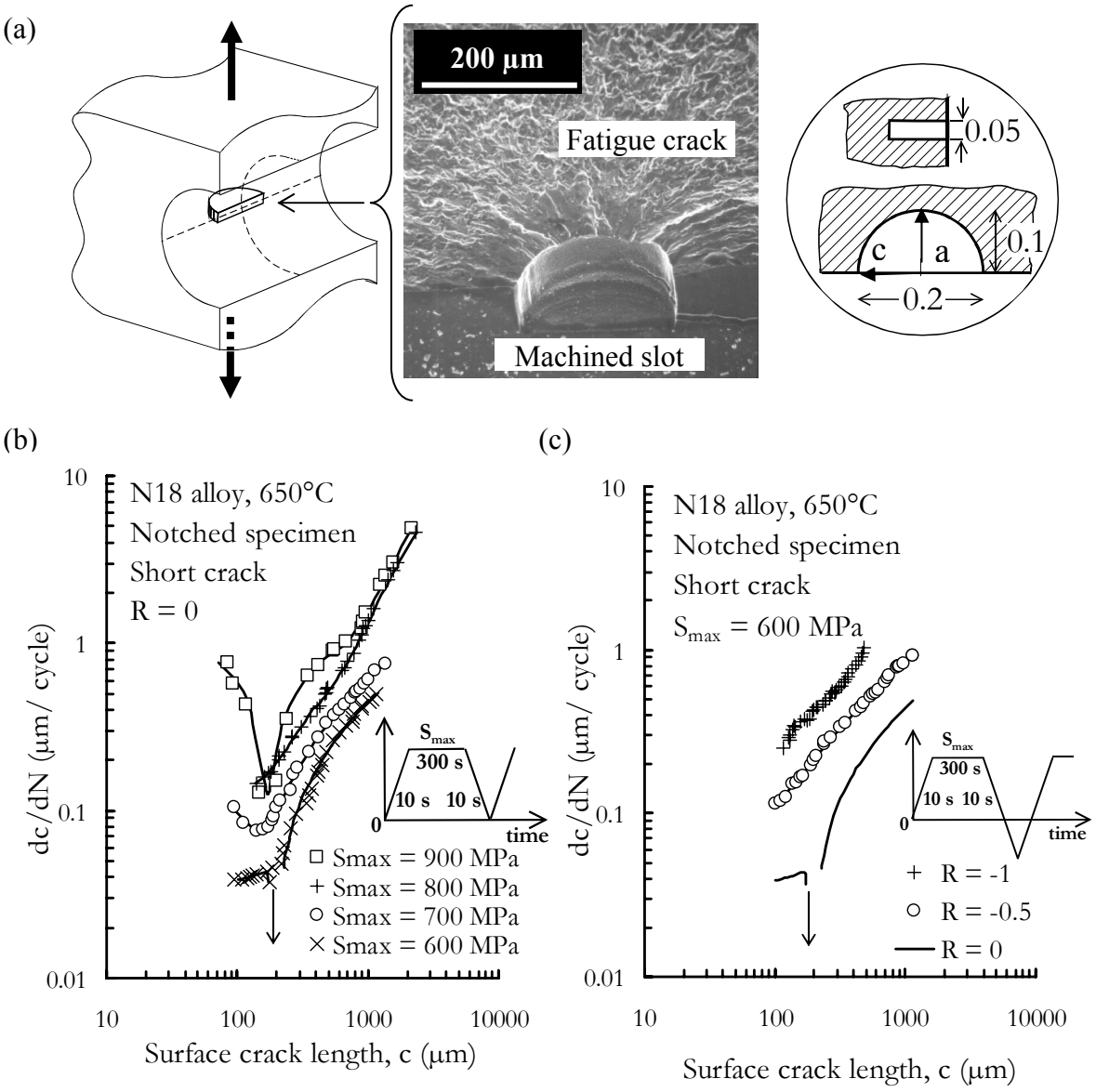

Fig. 1. Short crack growth rates measured in notched DEN specimens (N18 alloy at 650°C, cycles 10s-300s-10s): (a) semi-circular initial slot located at the center of the notch root. All dimensions in mm; (b) effect of maximum applied stress at R = 0; (c) effect of mean stress.

These results on short cracks were compared to the growth of long cracks measured on conventional unnotched specimens (KB2.5) containing a semicircular EDM defect of 0.3 mm in depth. On these specimens, a precracking was carried out at room temperature with a loading frequency of 10 Hz to obtain a semicircular crack with a depth of 0.5 mm. Fatigue crack growth tests were conduced at 650°C with trapezoidal cycles 10s-300s-10s and a load

ratio $R = S_{min}/S_{max}$ of 0.1 or 0.3. The crack growth rate was measured on these specimens for crack lengths up to 2 mm in depth using a potential drop technique. Further details of the experimental procedure in notched and unnotched specimens are given elsewhere [12].

Results

Typical results measured on notched specimens with R = 0 are shown in Fig. 1.b. Two stages of crack propagation were observed with these tests. The first stage corresponds to decreasing rates when surface crack lengths are less than 200 μm. Then above this critical crack length, a steady state of crack propagation is observed with increasing rates. The downtrend of the crack growth rate curves or short crack effect is more pronounced for a low applied load S_{max} of 600 MPa. For this load, the arrow in Fig. 1.b represents a crack growth rate less than 10^{-8} m/cycle occurring during the crack propagation. Moreover it is observed that lowering the R ratio from 0 to –1 overcomes the down trend effect; see Fig. 1.c. These results strongly suggest that short crack effects are linked to crack closure effects.

MODELLING AND DISCUSSION

Stress and strain fields at notch root and ΔK calculations

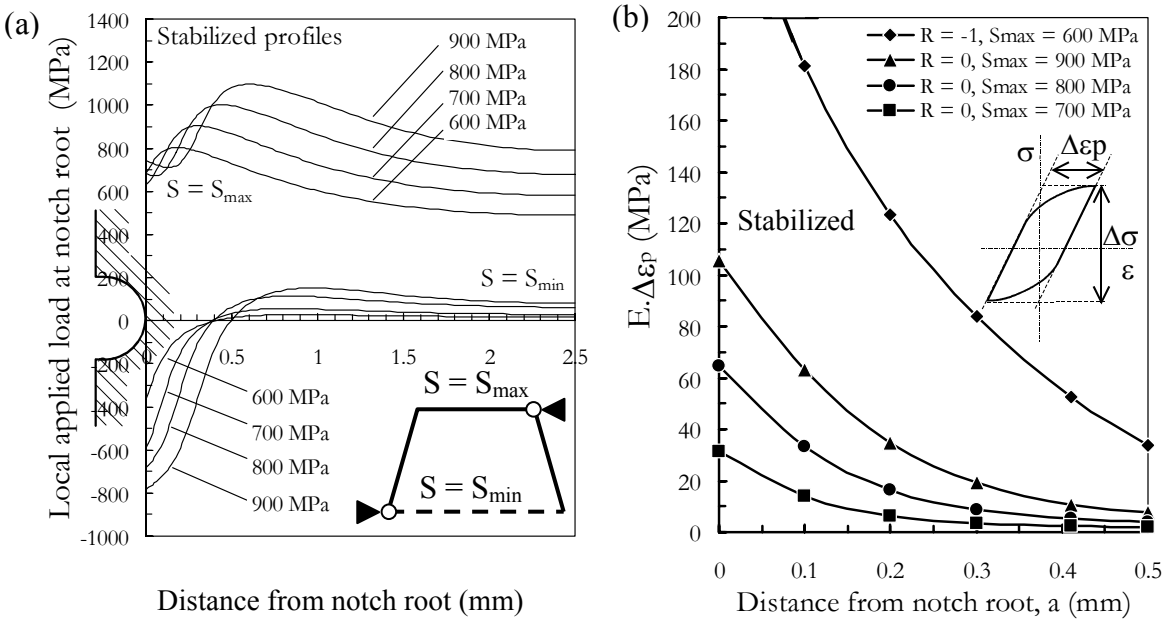

Fig. 2. Stabilized stress and strain profiles calculated at notch root with R = 0. Effect of applied loading: (a) on local stress at maximum load (S_{max}) and minimum load (S_{min}); (b) on pseudo-elastic stress calculated from plastic strain range.

The stress intensity range, ΔK, was calculated using the weight functions method introduced by Wang and Lambert [13,14], which was established for semi-elliptical cracks under non-uniform stress gradients. The local stress-strain field near the notch in the absence of a crack was calculated by Finite Element Method (FEM). The material behaviour was represented using an elasto-viscoplastic constitutive set of equations proposed by Lemaitre and Chaboche

[15]. The coefficients required for full identification of these equations, were identified using Low Cycle Fatigue tests performed at 650°C [11,12]. Detailed results of FEM calculations at notch root with cyclic loading are given in reference [12]. These FEM calculations showed that the tensile stress ahead of the notch progressively decreases to reach a stabilized condition, which was obtained after about 50 creep-fatigue cycles. Stabilized profiles at R = 0 with different applied loads are represented in Fig. 2.a. As expected, significant compressive stresses are noticed when the specimen is unloaded. This leads to an increase of the local applied stress range at notch root.

A simple correction to calculate ΔK accounting for the cyclic plasticity at notch root was used as proposed by Haigh and Skelton [16]. In this approach, the equivalent stress intensity range, ΔK^*, is calculated as:

$$\Delta K^* = (U.\Delta\sigma + E.\Delta\varepsilon_p).\sqrt{\pi a} \times F \quad (1)$$

where F is the LEFM geometry shape factor given by $F=\Delta K/(\Delta\sigma.\sqrt{\pi.a})$, Δσ is the total portion of the local stress range, U is the crack closure coefficient ($U=\Delta K_{eff}/\Delta K$), E is the Young's modulus and $\Delta\varepsilon_p$ is the plastic strain range in the vicinity of the notch. The pseudo-elastic stress, $E.\Delta\varepsilon_p$, calculated from stabilized profiles is represented in Fig. 2.b for different applied loads. For moderate applied stress ranges (<900 MPa), the strain range remains predominantly elastic. In this case, the calculated pseudo-elastic stress, $E.\Delta\varepsilon_p$, is less than 100 MPa. But for higher applied stress ranges (R = -1, S_{max} = 600 MPa), $E.\Delta\varepsilon_p$ can be larger than 200 MPa. However, the correction on ΔK given by equation (1) is less than 10% for this range when the crack depth is more than 90 μm. These calculations suggest that an elastic approach in terms of ΔK should apply in this situation, as indicated earlier [11]. Stress profiles at S_{max} and S_{min} similar to those shown in Fig. 2.a were approximated by a polynomial expression used in Wang and Lambert's results [13,14] to calculate both K_{max} and K_{min}. The results, which were used to compare the crack growth rates measured both on short cracks and on long cracks, are shown in the following.

Crack closure modelling and ΔK_{eff} calculations

In order to compare the crack growth rates of notched and unnotched specimens, the effective stress intensity factor, ΔK_{eff}, corresponding to these geometries must be determined first. In the present work, only plasticity-induced crack closure mechanisms will be considered. For unnotched specimens containing a semi-circular crack, closure effects are generally more pronounced near the surface than along the crack front within the specimen, due to the loss of constraint near the surface [17]. To investigate this effect on notched specimens, the current study utilises a simplified 2D FEM model to calculate the crack closure at the crack depth; see steps 1 and 2 in Fig. 3. Results of this model are then used in a 3D analytical simulation in order to calculate closure effects at the surface points of the crack; see steps 3 and 4 in Fig. 3. Both the 2D FEM model and the 3D analytical method will be explained in this section.

The 2D FEM model is based on a node-release technique similar to that proposed by Newman and Armen [18], which was used to simulate the growth of a fatigue crack in a 2D mesh. This technique was performed with the viscoplastic constitutive equations used previously to calculate the stress gradients in a uncracked geometry, as shown in Fig. 2.a. Plane strain conditions were assumed within the specimen. The mesh of a half-notched DEN specimen was

compared to unnotched geometry as shown in Fig. 4.a. In both meshes, the propagation area, also shown in this figure, was refined with 8-nodes quadratic elements. The size of the smallest element in this area is 20 μm. Crack propagation is simulated from 0.095 mm to 1 mm measured from the free surface. In this analysis, the release of one node corresponds to three loading cycles (10s-300s-10s). Nodes are released at the minimum load level. The initial crack length, a_0, is equal to the depth of the machined EDM slot (0.10 mm). This model calculates the crack opening ratio S_{op}/S_{max} of a 2D crack propagating in a notched specimen subjected to different applied loads and R ratios. The profile of the crack opening ratio as obtained from this 2D model is assumed in this study, to be similar to that experienced by the in-depth point along a 3D semi-elliptical crack.

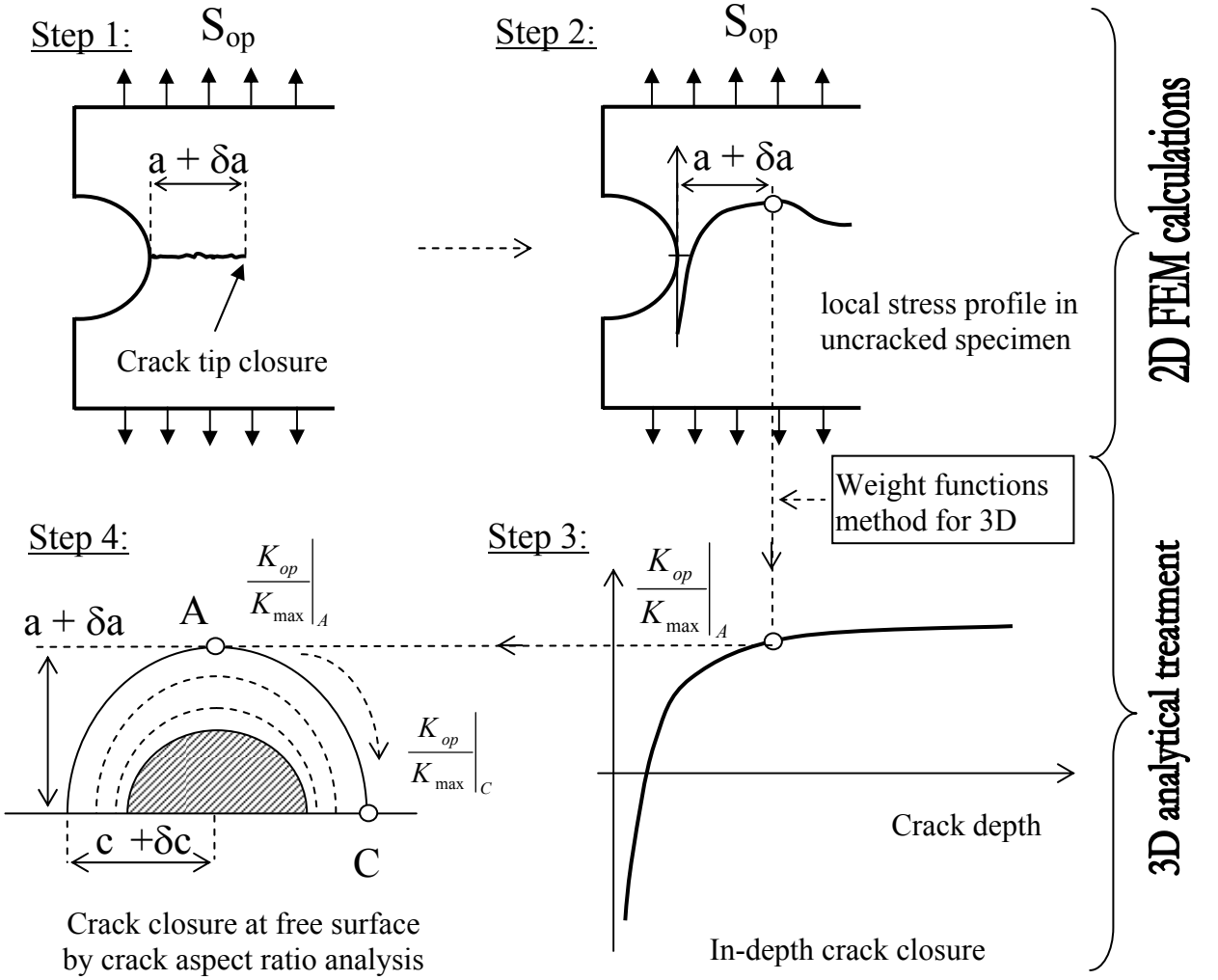

Fig. 3. Calculations of the opening stress intensity factor K_{op} for a semi-elliptical fatigue crack under non-uniform stress field, in-depth (A) and at free surface (C).

On the basis of this assumption, a procedure was established to determine the opening stress intensity factor, K_{op}, of a semi-elliptical crack under a stress gradient (steps 2 and 3 in Fig. 3). This procedure is described as follows. For a stress level equal to S_{op}, the stabilized stress profile at the notch root in a specimen without a crack is determined. The corresponding K_{op} is then calculated using Wang and Lambert's weight functions given at the deepest point of the crack front (point A). Figure 4.b shows the results of this procedure when S_{max} = 700 MPa and

R = 0 with a semi-circular crack front (a/c = 1). It is observed that the numerical results obtained on unnotched specimens are in good agreement with the experimental data for long cracks, as given in reference [10] (K_{op} = 0.24 K_{max}). Furthermore, the opening ratios between unnotched and notched specimens are very similar when the crack is long (>200 μm). However, the crack closure effect is significantly less pronounced with notched specimens when the crack is very small (<200 μm). This result is in agreement with those of Pommier et al. [8] and Clung and Sehitoglu [19] who showed that crack opening levels are small in the notch root vicinity and, then, increase rapidly and stabilize out of the notch field.

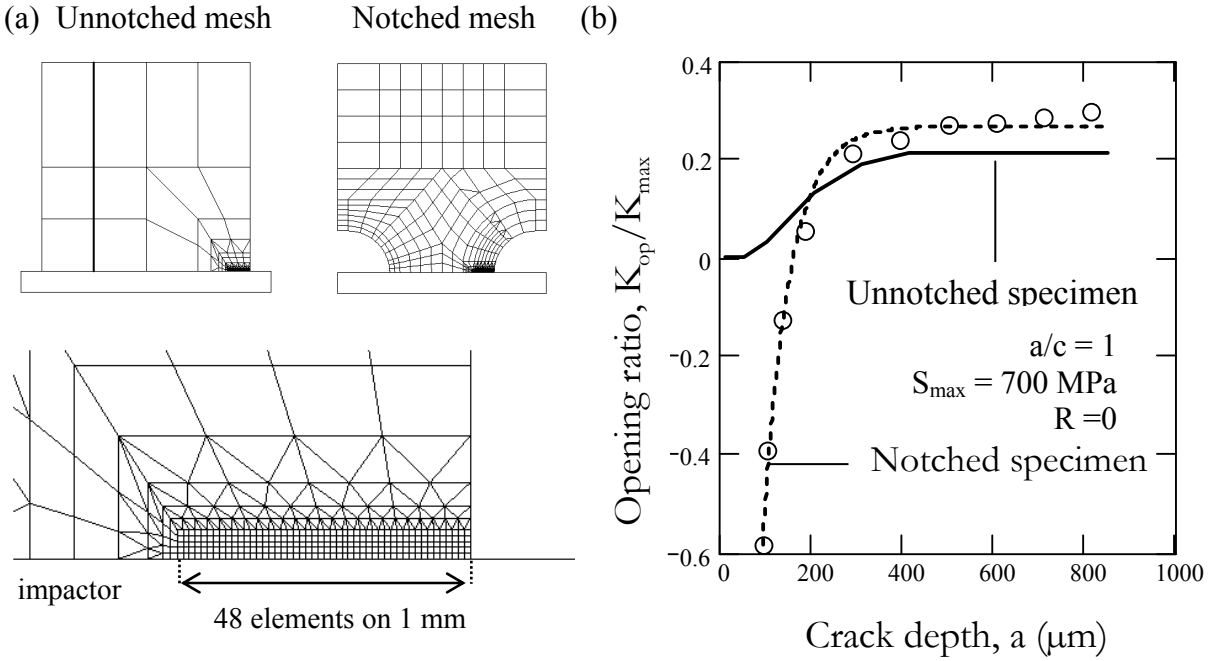

Fig. 4. 2D Finite Element calculations of crack closure: (a) geometry of unnotched and notched meshes used in the calculations; (b) final results K_{op} / K_{max} versus crack depth after analytical procedure.

The crack closure at the free surface (point C) was estimated from the knowledge of the opening ratios inside the specimens and using the method proposed by Jolles and Tortoriello [19]. In this technique, the crack growth increments at A and C, δa and δc respectively, are correlated as follows:

$$\delta a = \left(\frac{\Delta K_{eff,A}}{\Delta K_{eff,C}} \right)^n \times \delta c = \left(\frac{U_A \Delta K_A}{U_C \Delta K_C} \right)^n \times \delta c \qquad (2)$$

where n is the Paris's law exponent, U_A and U_C are the crack closure coefficients given at A and C, respectively. The method consists in the prediction of the crack aspect ratio, a/c, calculated iteratively from equation (2) imposing the shape of the initial defect. Figure 5 represents typical results obtained on DEN specimens tested with S_{max} = 900 MPa and R = 0. The analysis of the crack front shape obtained from interrupted tests as shown in this figure, indicates that the use of the ratio U_C/U_A = 1 is not a valid assumption. A correction to this

approach was the use of a procedure introduced by Jolles and Tortoriello [19], which is applied to fit the ratio U_C/U_A using experimental measurements of the crack front shape, as shown in Fig. 5. The ratio used in this figure is fitted into the form:

$$\frac{U_C}{U_A} = 0.55 + (1 - 0.55) \cdot \exp\left[-2 \cdot \frac{a - a_0}{t} \right] \tag{3}$$

where t is the thickness of the specimen (t = 5 mm) and a_0 is the initial crack depth. This result shows that crack closure effects are more important along the free surface than inside the specimen. Jolles et Tortoriello [19] reached similar conclusions from observations on unnotched specimens (U_C/U_A = 0.91). It can, however, be noticed that the difference in crack closure along the crack front is less significant in unnotched specimens than in notched ones. The difference between these two geometries can be related to the increase of local stress range in the vicinity of the notch. Further studies to validate equation (3) for different applied loads are necessary. In the present work, the effective stress intensity factor in C, $\Delta K_{eff,C}$, was calculated using equation (3) for notched DEN specimens and U_C/U_A = 0.9 for unnotched specimens.

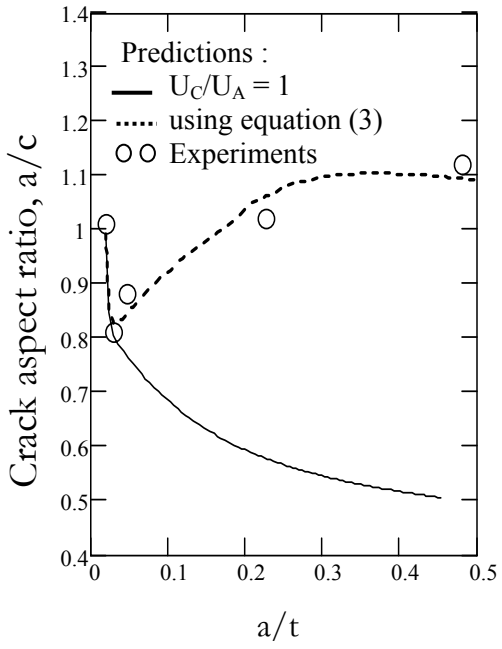

Fig. 5. Experimental examinations of crack front in notched specimens tested at 650°C with R = 0 and S_{max} = 900 MPa, and analytical predictions of crack aspect ratio.

Crack growth rate analysis

The crack growth rates obtained from notched specimens tested at 650°C are shown in Fig. 6. This figure includes also the results for long cracks obtained on conventional CT type specimens [10] and relatively long crack data obtained in this study using unnotched KB2.5 specimens. In Fig. 6.a, where no crack closure effect is considered, short and long cracks exhibit significant differences in crack growth behaviour at the free surface (point C), particularly at high ΔK values. It is also observed that a decreasing dc/dN pattern is present at

low values of ΔK. In this case, to calculate ΔK, it was assumed that a/c = 1, which is in good agreement with the experimental results shown in Fig. 5, at least when half surface crack lengths reached approximately 1 mm. Similar results, which are presented elsewhere [11], were obtained for in-depth crack growth rates (point A). Figure 6.b shows the results obtained considering the crack closure estimate presented in this paper. In this figure, it is observed that the short crack growth rates effects found in notched specimens at lower values of ΔK no longer exist when closure effects are properly taken into account. This methodology seems, therefore, to be efficient to assess the significance in lifetime predictions of the very early stage of crack propagation.

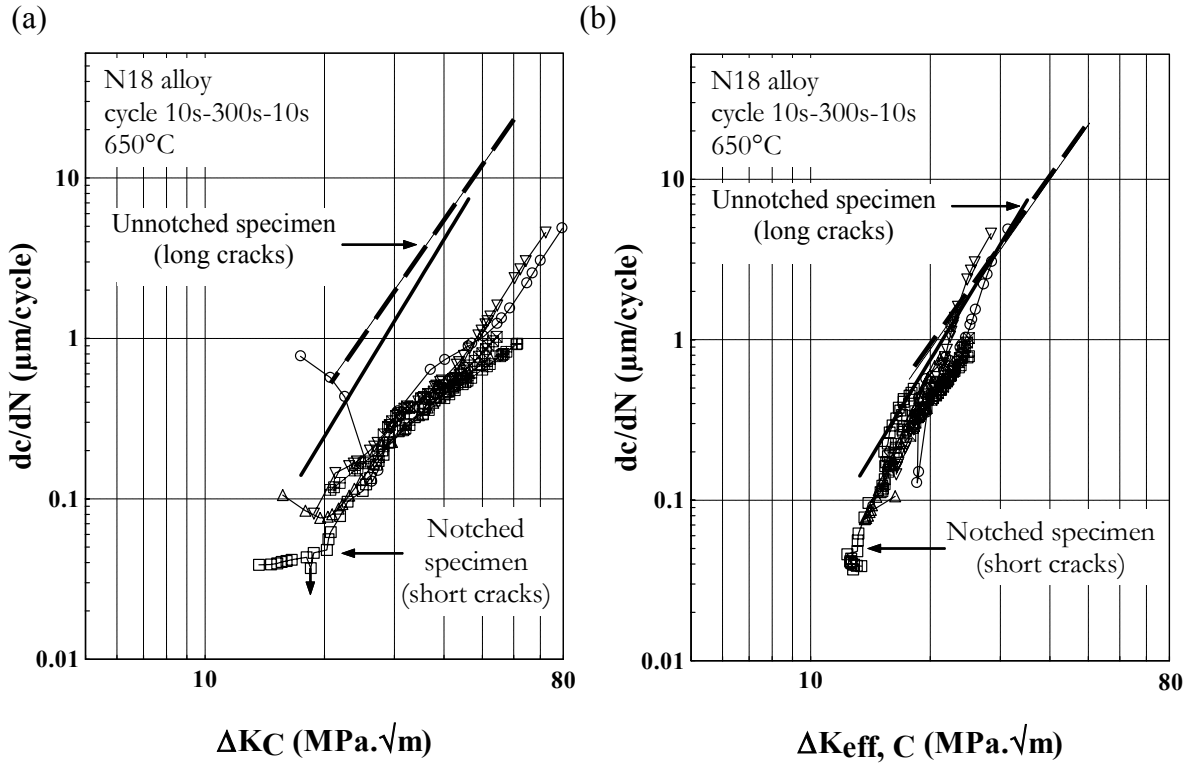

Long cracks / Unnotched specimen: KB2.5 ——— CT – – –

Short cracks / Notched specimen:

S_{max} =	0.5 σ_o	0.6 σ_o	0.7 σ_o	0.8 σ_o
R = 0	□	△	▽	○
R = -0.5	⊞			
R = -1	⊠			

Fig. 6. Comparison of fatigue crack growth rates measured in unnotched and notched specimens: (a) no crack closure is considered; (b) after 3D crack closure analysis.

CONCLUSIONS

1. The growth of short fatigue cracks was measured on N18 alloy at 650°C using DEN notched specimens. Typical downtrends of the crack growth rates were observed when R is equal to zero. This effect is no longer existent when negative R ratios are applied, keeping the same value for the maximum applied stress.

2. The stress intensity factor for a semi-elliptical crack and the crack opening were determined through FEM modelling using viscoplastic constitutive equations. A methodology was established in order to calculate the opening ratios within the specimen and at the free surface. It has been shown that crack closure effects calculated within the specimen are less pronounced in the vicinity of the notch root. However, the crack closure effect is more significant at the free surface than within the specimen. A phenomenological equation has been given to represent the change of crack closure along the crack in notched bodies. FEM calculations simulating the growth of a 3D crack from notches are necessary to extend these results.

3. Using the current methodology, it has been shown that the differences in growth between short and long cracks are simply interpreted by a mechanical effect related to crack closure effects. This methodology shows its ability to assess the significance of the early stage of propagation in lifetime predictions of turbine disks.

ACKNOWLEDGEMENTS: financial support from SNECMA is greatly acknowledged. Thanks also are due to Dr J.C. Lautridou from SNECMA and Prof. H. Ghonem from University of Rhode Island for many fruitful discussions and to Dr. J. Besson for his help in numerical calculations.

REFERENCES

1. S. Pearson (1975). *Engng Fracture Mech*. **7**, 235-247.
2. B. G. Journet, A. Lefrancois, and A. Pineau (1989). *Fatigue Fract. Engng Mater. Struct.* **12**, n°3, 237-246.
3. W. Elber (1971). ASTM STP 486, pp. 230-242.
4. R. A. Smith and K. J. Miller (1977). *Int. Journal of Mechanical Sciences* **19**, n°1, 11-22.
5. B. N. Leis (1985). *Engng Fracture Mech.* **22**, n°2, 279-293.
6. C. S. Shin and R. A. Smith (1988). *Engng Fracture Mech.* **29**, n°3, 301-315.
7. S. Pommier, C. Prioul, J. C. Lautridou and P. Bompard (1996). *Fatigue Fract. Engng Mater. Struct*. **19**, n°9, 1117-1128.
8. S. Pommier, C. Prioul and P. Bompard (1997). *Fatigue Fract. Engng Mater. Struct*. **20**, n°1, 93-107.
9. R. H. Van Stone, M. S. Gilbert, O. C. Gooden, and J. H. Laflen (1988). ASTM STP 969, T. A. Cruse Ed., Philadelphia, pp. 637-656.
10. A. Pineau (1997). In *Proc. of the Conf. "Engineering against fatigue"*. Eds J. H. beynon, M. W. Brown, R. A. Smith, T. C. Lindley and B. Tomkins. Sheffield (UK). 557-565
11. F. Sansoz, B. Brethes and A. Pineau (2001). To be published in *Fatigue Fract. Engng Mater. Struct.*
12. F. Sansoz (2000). *Ph.D. thesis*. Ecole des Mines de Paris
13. X. Wang and S. B. Lambert (1995). *Engng Fract. Mech*. **51**, n°4, 517-532.
14. X. Wang and S. B. Lambert (1997). *Engng Fract. Mech*. **57**, n°1, 13-24.
15. J. L. Chaboche and J. Lemaitre (1985). Mécanique des matériaux solides. Dunod, Bordas, Paris.
16. J. R. Haigh. and R. P. Skelton (1978). *Mater. Sci. Engng,* **36**, 133-137.
17. J. Z. Zhang and P. Bowen (1998). *Engng Fract. Mech.*, **60**, n°3, 341-360
18. J. C. Jr Newman and H. Jr Armen (1975). *AIAA journal*, **13**, n°8, 1017-1023
19. R. C. McClung and H. Sehitoglu (1989). *Engng Fract. Mech*., **33**, n°2, 237-252
20. M. Jolles and V. Tortoriello (1983). ASTM STP 791, pp. I-297-I-307